

Electron transfer emission in simple transition metal donor–acceptor systems

John F. Endicott *, Patrick G. McNamara, Tione Buranda ¹,
Ariel V. Macatangay

Department of Chemistry, Wayne State University, Detroit, MI 48202, USA

Received 17 September 1999; received in revised form 14 January 2000; accepted 26 January 2000

Contents

Abstract	62
1. Introduction	62
1.1 Summary of properties and characteristics of the CN [−] -bridged donor–acceptor complexes	63
2. Observations on the photoinduced electron transfer behavior of cyano-bridged donor–acceptor complexes in ambient solutions	65
2.1 General observations	65
2.2 Electron transfer luminescence at 77 K.	66
3. Interpretation and implications	69
3.1 Characteristics of the electron transfer emissions and their contrasts with (²E)Cr(III) emissions	69
3.2 Some implications of the emission energies	70
3.3 The possible origin of the ‘dual’ emission behavior.	71
3.4 Some implications of the electron transfer emission band shape	71
3.5 Implications of the large k_H/k_D ratios	73
4. Summary	74
Acknowledgements	74
References	74

Abbreviations: [14]aneN₄, 1,4,8,11-tetraazacyclotetradecane; ms-Me₆[14]aneN₄, 5,12-ms-5,7,7,12,14,14-hexamethyl-1,4,8,11-tetraazacyclotetradecane; [15]aneN₄, 1,4,8,12-tetraazacyclotetradecane.

* Corresponding author. Tel.: +1-313-5772607; fax: +1-313-5771377.

E-mail address: jfe@chem.wayne.edu (J.F. Endicott).

¹ Present address: Cancer Center and Department of Pathology, University of New Mexico, School of Medicine, Albuquerque, NM 87131, USA.

Abstract

Electron transfer luminescences have been found in a simple class of covalently linked, $\text{Cr}^{\text{III}}\text{--CN--Ru}^{\text{II}}$, transition metal complexes at 77 K in a DMSO/ H_2O glass. These emissions are broad, structureless and centered at about 850 nm. The emission lifetimes are on the order of 1 μs , and increase 16–26-fold upon perdeuteration of coordinated am(m)ines. The properties of the electron-transfer excited states are consistent with an inverted region, spin forbidden emission process. © 2000 Elsevier Science S.A. All rights reserved.

Keywords: Metal–metal emission; Marcus inverted region; Cyanide-bridged metals

1. Introduction

Electron transfer in the Marcus inverted region [1–3] can be treated as a non-radiative excited state relaxation process [3,4]. This description implies that an electron transfer excited state should exhibit characteristic excited state properties. Thus, when the energy gap is sufficiently large compared to the nuclear reorganizational energy, $|\Delta G^\circ| \gg \lambda_{\text{r}}$, it should be possible to detect an emission from the higher energy electron transfer state (the electron transfer excited state). Such emission spectra would be a unique source of information about the parameters intrinsic to the electron transfer process [5,6]. For this process, the emission energy maximum is given by Eq. (1),

$$h\nu_{\text{max}}^{\text{em}} = E^{00} - \lambda_{\text{r}} + \dots \quad (1)$$

where E^{00} is the energy difference between the zero-th vibrational levels of the ground and emitting excited state, and λ_{r} is the total vibrational energy necessary to generate the electronic excited state in the nuclear coordinates of the ground state. The intensity of emission as a function of emission energy (photons per molecule per unit time) is given by Eq. (2) [7]. Here n is the solvent refractive index, ν_{f} is the frequency

$$I(\nu_{\text{f}}) = \left(\frac{64\pi^4}{3h^3c^3} \right) n^3 \nu_{\text{f}} H_{\text{GE}}^2 (\Delta\mu_{\text{GE}})^2 (\text{FC}) \quad (2a)$$

$$(\text{FC}) = (4\pi\lambda_{\text{s}}k_{\text{B}}T)^{-1/2} \sum_{j=0}^{\infty} F_j \exp\left(\frac{-(\Delta G_{\text{BET}}^\circ + \lambda_{\text{s}} + h\nu_{\text{f}} + jh\nu_{\text{h}})^2}{4\lambda_{\text{s}}k_{\text{B}}T} \right) \quad (2b)$$

$$F_j = \left(\frac{S^j e^{-S}}{j!} \right); \quad S = \left(\frac{\lambda_{\text{h}}}{h\nu_{\text{h}}} \right) \quad (2c)$$

of the emitted photon of energy $h\nu_{\text{f}}$, λ_{s} is the reorganizational contribution for vibrational modes (mostly of the solvent) for which $h\nu_{\text{s}} < k_{\text{B}}T$, λ_{h} is the reorganizational contribution for vibrational modes with $h\nu_{\text{h}} \gg k_{\text{B}}T$, $\Delta\mu_{\text{GE}}$ is the difference between the ground (G) and excited (E) state dipole moments, $\Delta G_{\text{BET}}^\circ$ is the reaction free energy for the back electron transfer (BET) and it is assumed that a single, high frequency vibrational mode, ν_{h} , contributes to the band shape [7–9] so that

$\lambda_r = \lambda_s + \lambda_h$. The Franck–Condon term (FC) determines the spectral distribution of the emission band (via the quantity $h\nu_f + \Delta G_{\text{BET}}$). This approach has been exploited in the study of linked organic donors and acceptors [10], organic ion pairs [7] and the relaxation of metal-to-ligand charge transfer (MLCT) excited states of polypyridyl complexes [11–15]. The lack of observed metal-to-metal electron transfer emissions has made it impossible to use this approach for simple transition metal electron transfer systems.

The emission energy bandwidth is determined by several factors. Eq. (2) indicates that the solvent reorganizational energy, λ_s , is important among these factors. For example, absorption and emission bands are broader in solution than in the ordered environment of a crystal lattice. Much of this effect arises because the vertical energy difference between the ground and the electron transfer excited state depends on the solvation of the molecular species. In solution one expects a distribution of solvent environments, and each solvent environment will have a slightly different vertical energy, $(|\Delta G_{\text{GE}}^\circ| + \lambda_r)$ consistent with Eq. (1). The experimental values of both $\Delta G_{\text{GE}}^\circ$ and λ_s will correspond to the averages of the respective distributions, and there will be some net standard deviation, σ_g , of $(|\Delta G_{\text{GE}}^\circ| + \lambda_r)$ from the average values. For such a system, the exponential factor (FC) of Eq. (2) can be represented as a gaussian function if the bandwidth (proportional to the square root of the denominator of the exponential) is approximately as represented in Eq. (3).

$$\Delta\nu_{1/2} \sim [8 \ln 2(2k_{\text{B}}T\lambda_s)]^{1/2} + 2\sigma_g \quad (3)$$

We have found electron transfer emissions in a class of simple coordination complexes containing a transition metal electron transfer donor covalently linked to a transition metal acceptor. The emission behavior of these systems provides a unique perspective on the factors governing inverted region electron transfer rates.

1.1. Summary of properties and characteristics of the CN^- -bridged donor–acceptor complexes

The $\text{Cr}(\text{MCL})(\text{CN})_2^+$ complexes (MCL = an aliphatic tetraazamacrocyclic ligand) can be ruthenated to form 3-centered donor–acceptor D/A systems, $\text{Cr}(\text{MCL})(\text{CNRu}(\text{NH}_3)_5)_2^+$, in which the CN^- -mediated D/A electronic coupling is very strong. This is manifested in an intense visible absorption band, $\epsilon_{\text{max}} \cong 4 \times 10^3 \text{ cm}^{-1}/\text{per Ru(II)}$ with $\Delta\nu_{1/2} \sim 5 \times 10^3 \text{ cm}^{-1}$ [16–21]. This Ru(II)/Cr(III) MM'CT absorption is typically at about 500 nm [16–21]. The complexes are reasonably stable in deaerated solutions in the dark, and they can be stored as solids in the refrigerator under argon.

An estimate of λ_r may be obtained by means of a comparison to the $[(\text{bpy})_2\text{M}(\text{CNRu}(\text{NH}_3)_5)_2]^z+$ complexes. The MM'CT absorptions of the Ru(II)-centered ($z = 6$) and the Cr(III)-centered ($z = 5$) complexes are nearly identical in $h\nu_{\text{max}}$, ϵ_{max} and $\Delta\nu_{1/2}$. If we approximate E^{00} by the difference in electrode potentials for the D^+/D and A/A^- couples, $\Delta E_{1/2}$, then Eq. (4) (where F is Faraday's constant) may be used to estimate λ_r . For the Ru(II) centered complex,

$$h\nu_{\max}^{\text{abs}} = F\Delta E_{1/2} + \lambda_r + \dots \quad (4)$$

$\Delta E_{1/2} = 1.39$ V and $h\nu_{\max} = 14.5 \times 10^3 \text{ cm}^{-1}$ (in acetonitrile) [17]. This leads to $\lambda_r \cong 3.3 \times 10^3 \text{ cm}^{-1}$ in acetonitrile and about 4×10^3 in water. Owing to the similar spectroscopy of the Cr(III)- and Ru(II)-centered complexes, a value of $\lambda_r \cong (4-5) \times 10^3 \text{ cm}^{-1}$ is estimated for the MM'CT transitions of the former.

In the $[\text{trans-Cr}(\text{[14]aneN}_4)(\text{CNRu}(\text{NH}_3)_5)_2]^{5+}$ complex the MM'CT absorption maximum is at 500 nm, so with $\lambda_r \cong 4.5 \times 10^3 \text{ cm}^{-1}$, $E^{00}(\text{Q}_{\text{et}}) \cong 15.5 \times 10^3 \text{ cm}^{-1}$ for the spin allowed, vibrationally equilibrated (quartet $\text{Cr}^{\text{II}}(\text{CN}^-)\text{Ru}^{\text{III}}$) excited state (VEqES) in ambient aqueous solution (see Fig. 1). Note that this excited state correlates with low spin Cr(II) and that the implied $E_{1/2}(\text{}^4\text{Cr}^{\text{III}}/\text{}^3\text{Cr}^{\text{II}}) \sim -1.6$ V. Since $E^{00}(\text{Q}) \gg \lambda_r$, this system must be deep in the Marcus inverted region. The local Cr(II) excited state spin configurations in the lowest energy VEqES can be either triplet (low spin) or quintet (high spin). As noted above, the absorption characteristics make the quintet Cr(II) configuration unlikely for the initial, or Franck–Condon excited state since such a configuration involves the population of $\text{d}\sigma^*$ orbitals and would result in a much larger bandwidth as is observed for the MM'CT absorptions of the Co(III) and Rh(III) analogs [16–21]. The low spin Cr(II) configuration is expected to result in MM'CT bandwidths similar to those of $\text{Ru}^{\text{II}}/\text{Ru}^{\text{III}}$ transitions, and they would tend to be at relatively low energy for the dicyano-macrocyclic ligand complexes. This triplet Cr(II) configuration coupled

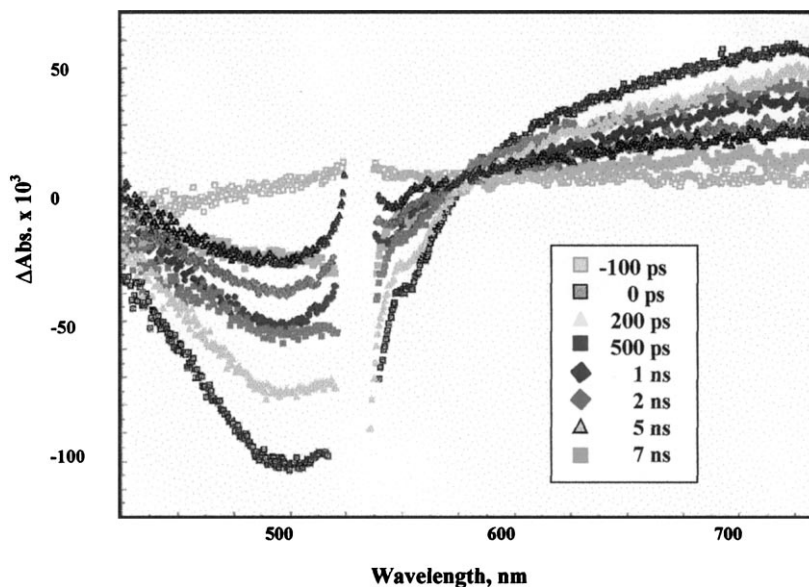


Fig. 1. Time resolved spectroscopic changes following the 532 nm excitation of the MM'CT absorption band of $[\text{trans-Cr}(\text{[14]aneN}_4)(\text{CNRu}(\text{NH}_3)_5)_2]^{5+}$ in ambient aqueous solution. The region of the pump beam at 532 nm has been deleted from the transient spectra.

with the CN^- -bridged, doublet Ru(III) gives rise to doublet and quartet electron transfer excited states. Whether the doublet or the quartet electron transfer excited state is lower in energy depends on the relative magnitudes of the magnetic coupling interactions. In a large number of CN -bridged paramagnetic metal complexes, the net local, M-CN-M' coupling is antiferromagnetic [22]. This seems most consistent with our observations, and we postulate a slightly lower energy for the ($^3\text{Cr(II)}/^2\text{Ru(III)}$) electron transfer excited state with doublet spin multiplicity. A value of $E^{00}(\text{Q}_{\text{et}}) \sim 14 \times 10^3 \text{ cm}^{-1}$ is plausible. These energy estimates are summarized in Fig. 2. If we assume similar values of λ_{r} for the $^3\text{Cr(II)}/^2\text{Ru(III)}$ quartet and doublet states, then an ambient emission would occur at about $9 \times 10^3 \text{ cm}^{-1}$. This would in principle be detectable. Both the intensity and the energy of such an emission should be larger at low temperatures. We have found that several of these complexes exhibit electron transfer emissions in frozen solutions. The synthesis and ground state properties of these complexes have been reported previously [16,17,23].

2. Observations on the photoinduced electron transfer behavior of cyano-bridged donor–acceptor complexes in ambient solutions

2.1. General observations

We find that well defined transients with 0.5–10 ns lifetimes are generated in ambient solutions following irradiations of several complexes of the type $\text{LA}(\text{CND})^{n+}$, where L is an aliphatic amine, $\text{D} = \text{Ru}(\text{NH}_3)_5^{2+}$ and $\text{A} = \text{Co}^{3+}$ or

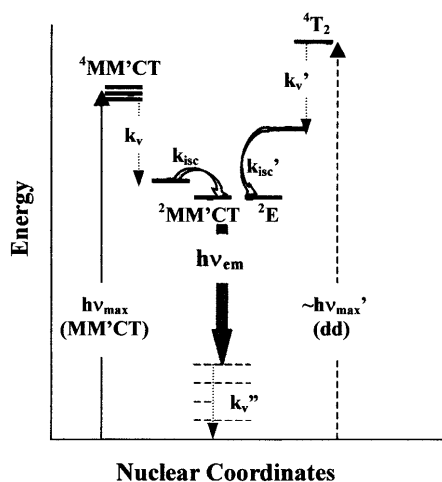


Fig. 2. Qualitative energy level diagram illustrating the relationships between possible excited states of the $[\text{trans-Cr}([14]\text{aneN}_4)(\text{CNRu}(\text{NH}_3)_5)_2]^{5+}$ complexes. The $\text{Ru(II)}/\text{Cr(III)}$ MM'CT states are on the left, Cr(III) metal centered states are on the right. The k_{v} are rate constants for vibrational relaxation within an electronic manifold, the k_{isc} are intersystem crossing rate constants for the crossings between electronic states of different spin multiplicities.

Cr^{3+} (e.g. see Fig. 1 [18,20]. For example, the transients generated by the irradiation of the $\text{Ru}^{\text{II}}/\text{M}^{\text{III}}$ MM'CT absorption band of the $\text{M}^{\text{III}}([\text{14}] \text{aneN}_4)-(\text{CNRu}^{\text{II}}(\text{NH}_3)_5)^{5+}$ complexes with $\text{M} = \text{Co}$ and Cr both exhibit $\geq 75\%$ bleaching of the ground state MM'CT absorbance and the formation of an excited state absorbance at about 600–700 nm. In both complexes the ground state absorbance recovered nearly completely (there is some photodecomposition, $< 10\%$, of both complexes during the pump and probe experiments), and the lifetime for its recovery was very close to that for the decay of the excited state absorbance. The transient behavior of these systems contrasts dramatically with the vibrationally excited, ultra short (~ 100 fs lifetimes) electron transfer excited state lifetimes characteristic of $(\text{NC})_5\text{D}(\text{CNA}(\text{NH}_3)_5)^-$ complexes in which D and A are combinations of Fe, Ru and Os [24–29]. The relatively long excited state lifetimes found for the CoCNRu and CrCNRu complexes are likely to be the consequence of very rapid intersystem crossing to generate electron transfer excited states with spin multiplicities different from those of the ground state [18,20]. Low energy excited states that differ in spin multiplicity are not possible for $\text{Ru}^{\text{II}}\text{CNRu}^{\text{III}}$ systems.

Several systems are compared in Table 1. The $\text{Cr}(\text{III})$ and $\text{Co}(\text{III})$ complexes (with tetraazamacrocyclic ‘spectator’ ligands) so far examined have lifetimes in aqueous solution that are in the ns time regime, roughly 10^4 longer lived than are the RuCNRu analogs. As noted above, the major qualitative contrast in these systems is that electronic states different in spin multiplicity are possible in the complexes with $\text{Cr}(\text{III})$ and the $\text{Co}(\text{III})$ centers, but not in the complexes with $\text{Ru}(\text{II})$ centers.

2.2. Electron transfer luminescence at 77 K

Irradiations of the MM'CT bands (band maxima at ~ 500 nm [16–21] of several $\text{LCr}(\text{CNRu}(\text{NH}_3)_5)^{n+}$ complexes in $\text{DMSO}/\text{H}_2\text{O}$ glasses at 80 K result in near-infrared luminescences with band maxima at 750–850 nm, Fig. 3 and Table 2. The reduced emission bands, $I(\nu_{\text{f}})_{\text{obsd}}/\nu_{\text{f}}$, are not gaussian. The change of intensity with frequency is more rapid on the high-energy side than on the low energy side of the emission maximum. In terms of Eq. (2), this implies that there are some contributions to (FC) from vibrational modes with $h\nu_{\text{h}} \sim 400\text{--}500\text{ cm}^{-1}$. The overall bandwidths vary from $\Delta\nu_{1/2} = 980\text{--}1500\text{ cm}^{-1}$ and decay lifetimes from $\tau = 0.8\text{--}1.4\text{ }\mu\text{s}$. Irradiations of the N-deuterated complexes in $\text{DMSO}/\text{D}_2\text{O}$ (80 K) result in much more intense emissions with the same bandwidths and $\tau = 16\text{--}82\text{ }\mu\text{s}$. The transient decays are probably multiphasic, but we have fitted them to bi-exponential decay functions. We have used these fits as the basis for estimating the mean lifetimes for the luminescence decays [30]: $\tau_{\text{m}}^{-1} = (A_1/\tau_1 + A_2/\tau_2)/(A_1 + A_2)$, where the A_i are the amplitudes from the biphasic fits. The observations are summarized in Table 2.

All the emissions from the CrCNRu complexes examined so far are excitation energy dependent. For example, emission band maxima increase $200\text{--}300\text{ cm}^{-1}$ and the lifetime increases about twofold for a $(2\text{--}3) \times 10^3\text{ cm}^{-1}$ increase in the

Table 1
MM'CT transient lifetimes, ground state absorption properties and excited state properties^a

Complex ^b	k_{bet} (obsd) (s ⁻¹)	$h\nu_{\text{max}}^{\text{abs}}$	ϵ_{max} ^c	$\Delta\nu_{1/2}$	$-\Delta G_{\text{DA}}^{\circ}$ ^d	λ_{vib} ^e	Ref.
<i>trans</i> -Cr ^{III} ([14]aneN ₄)(CNRu ^{II} (NH ₃) ₅) ₂ ⁵⁺	1.5×10^8	20.0	4000	4.9	~14	4.5	[16–19]
<i>trans</i> -Cr ^{III} ([15]aneN ₄)(CNRu ^{II} (NH ₃) ₅) ₂ ⁵⁺	nd	19.4	3550	4.6		4.	[16], this work
<i>trans</i> -Cr ^{III} (Me ₆ [14]aneN ₄)(CNRu ^{II} (NH ₃) ₅) ₂ ⁵⁺	0.8×10^8	19.4	3200	5.2		5	[16], this work
<i>trans</i> -Co ^{III} ([14]aneN ₄)(CNRu ^{II} (NH ₃) ₅) ₂ ⁵⁺	20×10^8	19.3	500	7.0	11.5	7.8	[16,19]
<i>cis</i> -Ru ^{II} (bpy) ₂ (CNRu ^{III} (NH ₃) ₅) ₂ ⁶⁺	$> 5 \times 10^{10}$	15.3	3880	5.0	11.2	4.5	[16,24]
<i>cis</i> -Cr ^{III} (bpy) ₂ (CNRu ^{III} (NH ₃) ₅) ₂ ⁵⁺	nd	15.5	3000	6.0	~14	5.5	[16]
Ru ^{II} (tpy)(bpy)(CNRu ^{III} (NH ₃) ₅) ₃ ³⁺	$> 5 \times 10^{11}$	14.3	4100	4.9	9.6	4.5	[16,26]
Ru ^{II} (CN) ₅ (CNRu ^{III} (NH ₃) ₅) ⁻	1×10^{13}	14.6	2500		~8	6.6	[25,27,28,44]

^a All energies in units of 10³ cm⁻¹; nd, not determined; ambient aqueous solutions.

^b Macrocyclic ligands (MCL) in abbreviations.

^c Absorptivity in 1 cm path length for a 1 M concentration.

^d Estimated from Eq. (7) and the difference of electrode potentials or a estimate of λ_{vib} .

^e Estimates referenced to *cis*-Ru^{II}(bpy)₂(CNRu^{III}(NH₃)₅)₂⁶⁺.

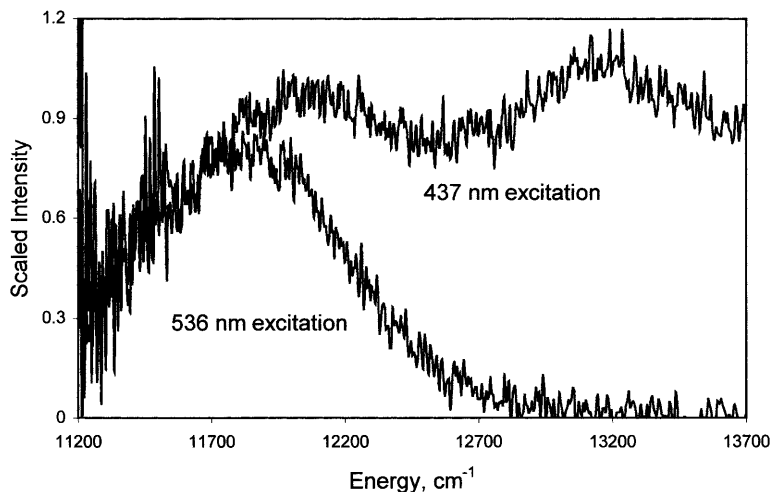


Fig. 3. The electron transfer emission from $[trans\text{-Cr}([14]\text{aneN}_4)(\text{CNRu}(\text{NH}_3)_5)_2]^{5+}$ in DMSO–H₂O glass at 77 K following excitation near the MM'CT absorption maximum (536 nm, lower curve) and at an energy greater than that of the MM'CT absorption (436 nm, lower curve).

excitation energy for irradiations of the $\text{Cr}(\text{NH}_3)_5(\text{CNRu}(\text{NH}_3)_5)^{4+}$ complex; this corresponds to irradiations through the MM'CT absorption band. For this complex, the increases of $h\nu_{\text{max}}^{\text{em}}(\text{obsd})$ and τ_{em} are weak sigmoidal functions of the excitation energy; i.e. both quantities increase as the excitation energy increases through the MM'CT absorbance maximum, then they approach a maximum value as the excitation energy increases beyond the MM'CT absorbance. We have resolved two emission bands, with maxima at 830 and 750 nm, for excitations of the $trans\text{-Cr}([15]\text{aneN}_4)(\text{CNRu}(\text{NH}_3)_5)_2^{5+}$ at about 410 nm, but only the 830 nm

Table 2

Comparison of electron transfer luminescence to d–d luminescence of several transition metal donor–acceptor complexes

Complex	λ_{max} (77 K) ^a nm	τ (77 K) ^b μs	$k_{\text{H}}/k_{\text{D}}$
$\text{Cr}(\text{NH}_3)_5(\text{CNRu}(\text{NH}_3)_5)^{3+}$	763	3	27
$\text{Cr}(\text{NH}_3)_5(\text{CN})_2^+$ ^c	680	100	75
$trans\text{-Cr}([14]\text{aneN}_4)(\text{CNRu}(\text{NH}_3)_5)_2^{5+}$	810	0.8	20
$trans\text{-Cr}([14]\text{aneN}_4)(\text{CN})_2^+$ ^c	717	361	13
$trans\text{-Cr}([15]\text{aneN}_4)(\text{CNRu}(\text{NH}_3)_5)_2^{5+}$	833	1.4	16
$trans\text{-Cr}([15]\text{aneN}_4)(\text{CN})_2^+$ ^c	711	278	
$trans\text{-Cr}(\text{Me}_6[14]\text{aneN}_4)(\text{CNRu}(\text{NH}_3)_5)_2^{5+}$	815	0.9	22
$trans\text{-Cr}(\text{Me}_6[14]\text{aneN}_4)(\text{CN})_2^+$ ^c	716	380	8

^a In DMSO–H₂O (50:50, v/v) glass at 77 K.

^b Values from irradiations of the low energy side of the MM'CT band (500–560 nm).

^c Data from Refs. [31–34].

emission was observed for excitation near to the DACT absorption maximum at 500 nm (see Fig. 3). A similar resolution of the two emission components has been achieved for the *trans*-Cr(Me₆[14]aneN₄)(CNRu(NH₃)₅)₂⁵⁺ complex. The resolved, high energy emission bands appear to have their electronic origins at about 100–200 cm⁻¹ lower energy than the origins of the ²E emissions of the parent dicyano complexes and they appear to exhibit some (poorly resolved) vibronic structure. The lifetimes of the ~ 750 nm components were appreciably (two to ten times) longer than those of the 830 nm components.

The high-energy emission bands are most reasonably assigned as ²E emissions of the electronically excited CrCNRu complexes. These emissions are somewhat broadened and shifted to slightly lower energies compared to those of the parent dicyano complexes [31–34], but this is expected for the ruthenated complexes. The new, lower energy, shorter lived and less structured emissions observed to follow irradiations of the MM'CT absorption bands are most plausibly assigned as metal–metal electron transfer emissions.

3. Interpretation and implications

The emissions described here as ‘electron transfer’ are the first such observed for a transition metal–transition metal relaxation process. The emission band structure can in principle provide unique information about the electron transfer reaction coordinate. The non-gaussian emission bands are consistent with Eq. (2), assuming that a high frequency vibrational mode, $h\nu_h$ in Eq. (2), contributes to the observed emission band and that $h\nu_h$ is not much greater than $4k_B T$ (at 80 K). This and related issues are discussed below. First we consider the assignment of the emission.

3.1. Characteristics of the electron transfer emissions and their contrasts with (²E)Cr(III) emissions

In Table 2 we compare the properties of the low energy emission bands of the ruthenated complexes to the ²E (d–d) emission of the cyanoam(m)inechromium(III) parent complexes [31–33]. The most striking contrasts are in the ratios of decay rates of the proteo forms of the complexes to the complexes in which all N–H functions have been replaced by N–D. For the ²E emissions k_H/k_D is nearly matrix independent and tends to increase with the number of N–H oscillators in the complex [33,34]. This is not the case for the low energy emissions discussed here. For these LCrCNRu complexes, k_H/k_D does not correlate in any way with the isotope effects in the parent complexes. It is pertinent that when the electron transfer excited state is much higher in energy (~ 1 eV) only a typical ²E emission is observed (at slightly lowered energy) in the (bpy)₂Ru(CN)(CNCr(NH₃)₃)³⁺ or (bpy)₂Ru(CNCr([14]aneN₄)(CN))₂⁴⁺ complexes [35,36]. In addition, we have examined the luminescence behavior of *trans*-Cr([15]aneN₄)(CNHg)₂⁵⁺ as a model for the behavior of the ligand field excited states when there is no mixing with electron transfer states. This complex exhibits a ‘typical’ (²E)Cr(III) emission, shifted to slightly higher energy and very slightly broadened compared to that of the parent.

The low energy emissions observed for the CrCNRu complexes are not consistent with the known features of (^2E)Cr(III) emissions [31–33,37,38], and they are much more characteristic of expectations for an electron transfer emission. We therefore assign them as electron transfer emissions.

The isotope effects are very large in the electron transfer systems described here. They contrast with $k_{\text{H}}/k_{\text{D}} < 2$ observed in organic ion pair electron transfer systems under ambient conditions [39]. The emission band shapes are not significantly altered by am(m)ine deuteration, but the distinct shift of the band to lower energy (by about $4\text{ cm}^{-1}/\text{N-H oscillator}$) is another contrast with the near independence of the (^2E)Cr(III) emission energy of am(m)ine deuteration. This shift in the emission band maximum probably has its origin in a difference of ground and excited state N–H force constants.

3.2. Some implications of the emission energies

Configurational mixing between the ^2E and the electron transfer excited states is likely in these complexes, and one expects rapid relaxation to the lowest energy electronic configurations. The relaxation in a frozen medium is something of a concern. Certainly some of the solvent reorganizational modes will be frozen out at 77 K [5]. If the matrix were absolutely rigid, then the emission maximum should be shifted from the absorption maximum only by $\lambda_{\text{h}} \ll \lambda_{\text{r}}$, an amount corresponding to the energy difference of the states of different spin multiplicity and some relatively minor electronic relaxation energies; not by the usual solution Stokes shift ($\sim 2\lambda_{\text{r}}$). We estimate that this should result in $h\nu_{\text{max}} \sim 18 \times 10^3\text{ cm}^{-1}$ for the electron transfer emission in a rigid matrix. That the observed emission maxima are at about $12 \times 10^3\text{ cm}^{-1}$ indicates that the situation for the systems considered here is more complicated. The energy difference between the excitation energy and the energy of the excited state PE minimum will appear in the medium as heat. The heat released for excitation at $20 \times 10^3\text{ cm}^{-1}$ when the PE minimum is at $15 \times 10^3\text{ cm}^{-1}$ is enough to increase the temperature of 50 solvent molecules by about 150 K. This is more than enough to melt the glass in the neighborhood of the molecule that absorbed the light. It is important to observe that most of the contributions to λ_{r} for these systems are expected to be in the solvent translations and rotations that correlate with the change of molecular dipole that accompanies electron transfer. One expects that the Franck–Condon state relaxation will take place over a few ps, while the diffusion of heat over a distance of several molecular diameters, away from the molecule, is expected to be a slower process. The resulting local melting will allow the electronically excited system to relax to near the PE minimum (estimated above to be at approximately $15 \times 10^3\text{ cm}^{-1}$). Heat flow away from the region of excitation will tend to freeze the solvent relaxation modes associated with the luminescence event (note that excited state lifetimes are in the order of nanoseconds, in ambient fluid solutions and this will allow time for appreciable cooling). These considerations are consistent with the observation that the observed values of $E^{00}(77\text{ K})$ are about the same as the value estimated above, for $E^{00}(300\text{ K})$, while the value of $\lambda_{\text{r}}(\text{eff})$ is much smaller at 77 than at 300 K.

3.3. The possible origin of the ‘dual’ emission behavior

The observed ‘dual’ emission is most likely attributable to the relaxation of the electronically excited complexes along different relaxation channels for excitation within the MMCT absorption band and for excitation at energies greater than this absorption. At the higher energy excitations we propose that the light absorption results in the population of a distribution of Franck–Condon electronic excited state configurations, and that different excited state configurations are biased towards relaxation along different channels. Since the higher energy excitations are at the wavelengths of the lowest energy, spin-allowed d–d absorption of the Cr(III) center (400–475 nm), these systems behave as if the different Franck–Condon excited states relax within the manifold of the predominant electronic configuration and that the crossing between manifolds is slow enough near the potential energy minima that the freezing solvent can trap the system in one or the other configuration. It is probably relevant that the d–d excitation of Cr(III) implicates largely molecular vibrational modes while electron transfer excitation of the CrCNRu moieties implicates largely solvent modes.

3.4. Some implications of the electron transfer emission band shape

The non-radiative relaxation of an electronic excited state or of an inverted region electron transfer system is generally expected to be temperature dependent in the classical limit when $h\nu_h \ll 4k_B T$. Even when $h\nu_h > 4k_B T$ the relaxation rate can be temperature dependent in a fluid medium [4,12,40,41]. In this high temperature regime the relaxation behavior is commonly fitted to an equation such as Eq. (5). This equation is very

$$k_{\text{BET}} = \left(\frac{4\pi^3 H_{\text{GE}}^2}{h^2 \lambda_s k_B T} \right) \sum_{j=0}^{\infty} F_j \exp \left\{ \frac{-(\Delta G_{\text{BET}}^\circ + \lambda_s + jh\nu_h)^2}{a^2} \right\} \quad (5)$$

similar to the expression for the radiative process given in Eq. (2), except that we have used $a = \Delta\nu_{1/2}/[2(\ln 2)^{1/2}]$ for a gaussian function and $\Delta\nu_{1/2}$ defined as in Eq. (3). The other parameters have been defined above. When $k_B T$ is sufficiently small, or if no low frequency modes contribute to λ_s ($\lambda_s = 0$) and if $\Delta G_{\text{BET}}^\circ$ is a single-valued parameter (i.e. independent of the solvation environment; we use E_{ij}^{00} for this single value of $\Delta G_{\text{BET}}^\circ$), then Eq. (5) no longer applies. The relaxation rate in this limit depends largely on vibrational overlap and Eq. (6) is often used [40,42].

$$k_{ij}^\circ = (H_{ij}^2/h)[8\pi^3/h\nu_h E_{ij}^{00}]^{1/2} [\exp(-\gamma E_{ij}^{00}/h\nu_h)] \quad (6a)$$

$$\gamma = \ln(E_{ij}^{00}/\lambda_h) - 1 \quad (6b)$$

However, in the present systems we expect that there is a range of values of $\Delta G_{\text{BET}}^\circ$, as a consequence of a distribution of solvates, so that $\Delta\nu_{1/2} \sim 2\sigma_g$, in the low temperature limit based on Eq. (3). For the systems considered here it is more useful to recast Eqs. (5) and (6) into the more general form of Eq. (7) in which

$$k_{\text{BET}} = \nu_{\text{h}}^{\text{c}} \sum_{j=0}^{\infty} F_j e^{-g_j^2/a^2} + \dots \quad (7)$$

$g_j = (\Delta G_{\text{BET}}^{\circ} + \lambda_{\text{s}} + j h \nu_{\text{h}})$ and $\nu_{\text{h}}^{\text{c}}$ is the crossing frequency in the limit of maximum vibrational overlap (note that $\nu_{\text{h}}^{\text{c}}$ contains the contributions of the electronic matrix element). In principle, Eq. (7) should be summed over all contributing vibrational modes, ν_{h} , and there may be higher order contributions corresponding to the simultaneous population of two different contributing vibrational modes. Values for a can be based on the observed bandwidths of the vibronic components of the emission. Thus, if we assume that the observed electron transfer emissions are properly resolved into two vibronic components, then $\Delta \nu_{1/2}(\text{obsd}) \sim 800 \text{ cm}^{-1}$. For $\Delta G_{\text{BET}}^{\circ} \cong 13 \times 10^3 \text{ cm}^{-1}$, $\lambda_{\text{s}} \cong 0$, $h \nu_{\text{h}} \cong 3200 \text{ cm}^{-1}$ and $j = 4$, $g_j \sim 0$. The magnitude of $\nu_{\text{h}}^{\text{c}}(\text{NH})$ can be estimated from the pre-exponential factor of Eq. (6) or from the pre-exponential factor of Eq. (2b) with $\Delta \nu_{1/2}(\text{obsd})/[2(\ln 2)^{1/2}]$ substituted for $(4\lambda_{\text{s}}k_{\text{B}}T)$; these approaches are reasonably consistent and give values of $\nu_{\text{h}}^{\text{c}}(\text{NH})$ in the range of $(H_{\text{GE}}^2 \times 10^{8 \pm 1}) \text{ s}^{-1}$. Since $k_{\text{BET}}(\text{obsd}) \sim 10^6 \text{ s}^{-1}$, $H_{\text{GE}}^2 F_j$ must be of the order of $10^{-2 \pm 1}$ in order for any equation such as Eq. (7) to be applicable. If one assumes that Eq. (7) is strictly applicable to these systems and that the NH and ND stretches are the dominant acceptor modes, then the isotope effect, $k_{\text{BET}}(\text{NH})/k_{\text{BET}}(\text{ND}) = 22$ is reasonably consistent with $\lambda_{\text{h}} \sim 3200 \text{ cm}^{-1}$ and $H_{\text{GE}} \sim 10^2 \text{ cm}^{-1}$. A smaller value of H_{GE} for the back electron transfer (and emission) than for the absorption (for which $H_{\text{GE}} \sim 3 \times 10^3 \text{ cm}^{-1}$ [17]) is reasonable for a spin forbidden back electron transfer process.

In the preceding analysis we have used Eq. (7) in a manner that would require the observed emission component to correspond to $j = 0$ in Eq. (3). This would result in a gaussian band shape if the only high frequency mode were the N–H stretch. That this is not the case suggests that some other vibrational mode $h\nu'_{\text{h}} > k_{\text{B}}T$ also contributes to the emission band shape. A progression in a vibrational mode $h\nu'_{\text{h}} \sim 500 \text{ cm}^{-1}$ with the $j' = 0$ contribution most strongly weighted could account for the band shape. This would be consistent with a small distortion ($\lambda'_{\text{h}} < \sim 300 \text{ cm}^{-1}$) in metal–ligand bond lengths accompanying electron transfer. The rate constant as represented in Eqs. (5) or (7) is insensitive (the exponent is near zero) to the details of contributions from any but the highest frequency vibrational modes. However, these details are far more evident in the emission band shape, since the observed emission band must correspond to a single component of any progression in the highest frequency mode (the $j = 1$ component in the N–H stretch is predicted to occur at about $9 \times 10^3 \text{ cm}^{-1}$, outside the range of our detector). The signal-to-noise and resolution levels of our measurements, and the intrinsic bandwidths of the emissions have not allowed us to clearly resolve the contributions of vibrational modes $h\nu'_{\text{h}} \ll h\nu_{\text{h}}$ or to make the resulting small corrections in the estimates of rate parameters based on Eq. (5). Nevertheless, it is clear that the use of an average frequency for ν_{h} (i.e. an average of 3200 and 500 cm^{-1} in the above analysis) would lead to a poor description of the observations, as noted elsewhere [41].

3.5. Implications of the large k_H/k_D ratios

Since there are a large number of N–H oscillators (at least 15–19) in the electron transfer systems considered here, this might be the origin of the very large isotope effects observed. However, as noted above, the k_H/k_D ratios for the Cr(III) parent 2E emissions are generally proportional to the number of N–H oscillators [33,37]. Since the summation over degenerate modes in Eqs. (5) or (7) is equivalent to multiplying by the number of degenerate modes (this factor is contained in γ in Eq. (6) [40]), the origin of the contrast is an issue. The contrast of the dependence of k_H/k_D for the (2E)Cr(III) and the electron transfer emissions on the number of N–H oscillators may originate from: (1) a similar number of N–H acceptor modes in all the electron transfer systems (e.g. the ammine ligand of Ru(III) in the excited state may dominate the relaxation process in the electron transfer systems); (2) the N–D vibrational modes are viable acceptor modes for the electron transfer systems, but not for the (2E)Cr(III) relaxation (it has been postulated that the proportionality of k_H/k_D to the number of NH oscillators for Cr(III) systems arises because the N–D modes are not good acceptor modes [33]). The information currently available does not allow us to determine which of these is most likely. While Eqs. (5–7) adequately account for the luminescence lifetime, these equations are very approximate, and possibly not entirely appropriate treatments of the observations. The assumption in Eqs. (3), (5) and (6) that only one high frequency mode contributes to the excited state relaxation and that this mode is equally weighted in Eqs. (3) and (5) is clearly not consistent with the observations, since we find that the NH modes dominate the low temperature non-radiative relaxation and there is evidence that a much lower energy mode, possibly a metal–ligand skeletal mode, is important in determining the emission band shape. In addition, the assumption intrinsic to Eqs. (3), (5), (6) and (7) that the pertinent force constants are the same in the ground and the excited state is apparently not correct in these systems.

Both Eqs. (5) and (6) assume similar vibrational frequencies in the ground and excited states. The clear difference, $\sim 80\text{ cm}^{-1}$, in emission band maxima of proteo- and deutero complexes suggests a zero point energy difference resulting from such a difference of vibrational frequencies. That the band maxima are at higher energies for the deutero complexes indicates a smaller force constant for the coupled N–H vibrations in the excited state. The limits represented in Eqs. (5–7) suggest that the highest frequency vibrational modes should dominate the low temperature nonradiative relaxation rate (note that $(\Delta G^\circ + \lambda_s + j\hbar\nu_h) \sim 0$). These vibrational modes are not necessarily the modes correlated with the largest distortion [40,41,43]. The analysis presented above indicates that the highest frequency modes, the vibrational modes that dominate the non-radiative relaxation rate, contribute less than 10% of the ambient reorganizational energy. That low temperature limiting models of the excited state relaxation rate can sometimes be based on emission band shapes [11–15] is not a necessary consequence of the theory.

4. Summary

The CrCNRu complexes have demonstrated that the low temperature rates of back electron transfer in the Marcus inverted region depend very strongly on the rate of disposition of excess energy. This is a remarkable example of a strongly allowed chemical process whose rate is limited by the constraints on the dissipation of the energy associated with the reaction process.

Acknowledgements

The authors thank the Office of Basic Energy Sciences of the Department of Energy for partial support of this research. We are grateful to the Center for Photoinduced Charge Transfer at the University of Rochester for access to their picosecond flash photolysis system. We are also grateful to Professor M.W. Perkovic for lending us the calibrated tungsten lamp.

References

- [1] R.A. Marcus, *Discuss. Faraday Soc.* 29 (1960) 21.
- [2] R.A. Marcus, *Annu. Rev. Phys. Chem.* 15 (1964) 155.
- [3] R.A. Marcus, *J. Phys. Chem.* 93 (1989) 3078.
- [4] N. Kestner, J. Logan, J. Jortner, *J. Phys. Chem.* 64 (1974) 2148.
- [5] R.A. Marcus, *J. Phys. Chem.* 94 (1990) 4963.
- [6] D.V. Matyushov, B.M. Ladanyi, *J. Phys. Chem. B* 102 (1998) 5027.
- [7] I.R. Gould, D. Noukakis, G.-J. Luis, R.H. Young, J.L. Goodman, S. Farid, *Chem. Phys.* 176 (1993) 439.
- [8] A.B. Myers, in: A.B. Myers, T.R. Rizzo (Eds.), *Laser Techniques in Chemistry*, vol. XXIII, Wiley, New York, 1995, p. 325.
- [9] A. Myers, *Acc. Chem. Res.* 30 (1998) 519.
- [10] H. Oevering, J.W. Verhoeven, M.N. Paddon-Row, J.M. Warman, *Tetrahedron* 45 (1989) 4751.
- [11] J.V. Casper, T.J. Meyer, *Inorg. Chem.* 22 (1983) 2446.
- [12] D. Graff, J.P. Claude, T.J. Meyer, in: S.S. Isied (Ed.), *Electron Transfer in Organometallic and Biochemistry*, ACS Advances in Chemistry Series No. 253, American Chemical Society, Washington, DC, 1997, p. 183.
- [13] E.M. Kober, J.V. Casper, R.S. Lumpkin, T.J. Meyer, *J. Phys. Chem.* 90 (1986) 3722.
- [14] Z. Murtaza, A.P. Zipp, L.A. Worl, D.K. Graff, W.E. Jones Jr., W.D. Bates, T.J. Meyer, *J. Am. Chem. Soc.* 113 (1991) 5113.
- [15] Z. Murtaza, D. Graff, A.P. Zipp, L.A. Worl, W.E. Jones Jr., W.D. Bates, T.J. Meyer, *J. Phys. Chem.* 98 (1994) 10 504.
- [16] M.A. Watzky, J.F. Endicott, X. Song, Y. Lei, A.V. Macatangay, *Inorg. Chem.* 35 (1996) 3463.
- [17] M.A. Watzky, A.V. Macatangay, R.A. Van Camp, S.E. Mazzetto, X. Song, J.F. Endicott, T. Buranda, *J. Phys. Chem.* 101 (1997) 8441.
- [18] J.F. Endicott, M.A. Watzky, A.V. Macatangay, S.E. Mazzetto, X. Song, T. Buranda, in: A.A. Kornyshev, M. Tosi, J. Ulstrup (Eds.), *Electron and Ion Transfer in Condensed Media*, World Scientific, Singapore, 1997, p. 139.
- [19] J.F. Endicott, M.A. Watzky, X. Song, T. Buranda, *Coord. Chem. Rev.* 159 (1997) 295.
- [20] J.F. Endicott, X. Song, M.A. Watzky, T. Buranda, *J. Photochem. Photobiol. A: Chem.* 82 (1994) 181.

- [21] J.F. Endicott, X. Song, M.A. Watzky, T. Buranda, *Chem. Phys.* 176 (1993) 427.
- [22] S.-i. Ohkoshi, O. Sato, T. Iyoda, A. Fujishima, K. Hashimoto, *Inorg. Chem.* 36 (1997) 268.
- [23] A.V. Macatangay, S.E. Mazzetto, J.F. Endicott, *Inorg. Chem.* 38 (1999) 5091.
- [24] P.F. Barbara, J.J. Meyer, M. Ratner, *J. Phys. Chem.* 100 (1996) 13 148.
- [25] T. Buranda, Y. Lei, J.F. Endicott, *J. Am. Chem. Soc.* 114 (1992) 6916.
- [26] S.K. Doorn, R.B. Dyer, P.O. Stoutland, W.W. Woodruff, *J. Am. Chem. Soc.* 115 (1993) 6398.
- [27] A. Ponce, M. Bachrach, P.J. Farmer, J.R. Winkler, *Inorg. Chim. Acta* 243 (1996) 135.
- [28] D.A.V. Tominaga, A.E. Kliner, A.E. Johnson, N.E. Levinger, P.F. Barbara, *J. Chem. Phys.* 98 (1993) 1228.
- [29] P.J. Reid, C. Silva, P.F. Barbara, L. Karki, J.T. Hupp, *J. Phys. Chem.* 99 (1995) 2609.
- [30] S.A. Trammell, J.A. Moss, J.C. Yang, B.M. Nakhle, C.A. Slate, F. Odobel, M. Sykora, B.W. Erickson, T.J. Meyer, *Inorg. Chem.* 38 (1999) 3665.
- [31] R.B. Lessard, J.F. Endicott, M.W. Perkovic, L.A. Ochrymowycz, *Inorg. Chem.* 28 (1989) 2574.
- [32] R.B. Lessard, M.J. Heeg, T. Buranda, M.W. Perkovic, C.L. Schwarz, Y. Rudong, J.F. Endicott, *Inorg. Chem.* 31 (1992) 3091.
- [33] C.K. Ryu, R.B. Lessard, D. Lynch, J.F. Endicott, *J. Phys. Chem.* 93 (1989) 1752.
- [34] J.F. Endicott, M.W. Perkovic, M.J. Heeg, C.K. Ryu, D. Thompson, in: S.S. Isied (Ed.), *Electron Transfer in Inorganic and Bioinorganic Chemistry*, ACS Advances in Chemistry Series No. 253, American Chemical Society, Washington, DC, 1997, p. 199.
- [35] C.A. Bignozzi, O. Bortolini, C. Chiorboli, M.T. Indelli, M.A. Rampi, F. Scandola, *Inorg. Chem.* 31 (1992) 172.
- [36] J.F. Endicott, R.B. Lessard, Y. Lei, C.K. Ryu, in: V. Balzani (Ed.), *Supramolecular Photochemistry*, Reidel, Dordrecht, 1987, p. 167.
- [37] J.F. Endicott, T. Ramasami, R. Tamilarasan, R.B. Lessard, C.K. Ryu, G.B. Brubaker, *Coord. Chem. Rev.* 77 (1987) 1.
- [38] L.S. Forster, *Chem. Rev.* 90 (1990) 331.
- [39] I.R. Gould, S. Farid, *J. Am. Chem. Soc.* 110 (1988) 7883.
- [40] R. Englman, J. Jortner, *Mol. Phys.* 18 (1970) 145.
- [41] K.F. Freed, J. Jortner, *J. Chem. Phys.* 52 (1970) 6272.
- [42] M. Bixon, J. Jortner, J. Cortes, H. Heilte, M.E. Michel-Beyerle, *J. Phys. Chem.* 98 (1994) 7289.
- [43] J.B. Birks, *Photophysics of Aromatic Molecules*, Wiley-Interscience, New York, 1970.
- [44] V.G. Pouloupoulou, H. Taube, F. Nunes, *Inorg. Chem.* 38 (1999) 2844.